Non-steady-state photoelectromotive force effect under linear and periodical phase modulation: application to detection of Doppler frequency shift

S. Mansurova,[1,*] P. Moreno Zarate,[1] P. Rodriguez,[1] S. Stepanov,[2] S. Köber,[3] and K. Meerholz[3]

[1]*Instituto Nacional de Astrofísica, Óptica y Electrónica, Apartado Postal 51 y 216, Puebla 72000, Mexico*

[2]*Centro de Investigación Cientifica y de Educación Superior de Ensenada, km.107 carretera Tijuana-Ensenada, Ensenada 22860, Mexico*

[3] *Department of Chemistry, University of Cologne, Luxemburger Strasse 116, 50939 Cologne, Germany*

**Corresponding author: smansur@inaoep.mx*

Received April 29, 2011; revised August 22, 2011; accepted August 31, 2011;
posted December 9, 2011 (Doc. ID 145202); published January 30, 2012

Non-steady-state photoelectromotive force effect in the presence of periodical and linear phase shift was investigated both theoretically and experimentally. It was shown that superposition of oscillating and linear movements of the interference pattern leads to the appearance of the sharp peak in the frequency dependence of the photoelectromotive force output current when the frequency of periodical modulation matches the frequency of the linear phase shift. We demonstrated experimentally that this effect can be used for determination of a Doppler frequency shift between signal and reference beam.

OCIS codes: 120.1088, 280.3340, 160.4890.

In recent years, detectors based on the non-steady-state photoelectromotive force (photo-emf) effect [1] have attracted significant attention for the detection of optical signals modulated in phase [1–3]. The photo-emf effect consists in the generation of an electrical current through a short-circuited photoconductive sample when it is illuminated by a dynamic interference pattern. This current is a result of the interaction of the relatively stable distribution of space charge electric field E_{sc} (caused by the charges trapped in the deep trapping centers) and the mobile distribution of free carriers. There are two basic configurations: the dc photo-emf excited by an interference pattern moving at constant velocity ("running" grating), which results in a dc current flowing through the sample [4]; and the ac photo-emf, which appears due to a periodically oscillating interference pattern and is measured as an ac component [5].

One application that is of interest in aerodynamics, fluid mechanics, and biomedical applications is the remote detection of the Doppler frequency shift Ω_L between two mutually coherent beams [the reference (R) and the signal (S) beams]. It was demonstrated earlier [6,7] that dc photo-emf can be used for this purpose. In this configuration the amplitude of the output signal is proportional to the fringe velocity, so the Doppler frequency shift can be evaluated by measuring the absolute value of the dc current flowing through the sample. Although the dc photo-emf configuration allows detection of the velocity without stringent alignment conditions, its profound drawback relies on the fact that the response of the detector is strongly dependent on the average light intensity, i.e., continuous calibration is needed in order to determine the value of Ω_L.

Here we report a new velocimeter scheme based on the combination of both ac and dc photo-emf configurations, i.e., when the dynamics of the illuminating interference pattern is determined by the superposition of a linear and a periodical phase modulation. We demonstrated, both theoretically and experimentally, that the periodical modulation (at frequency Ω_P) can be used as a probe to determine the frequency of the linear modulation Ω_L.

The proposed method can be analyzed by considering illumination of the short-circuited photoconductor by an interference pattern with the following intensity distribution:

$$I(x) = I_0[1 + m\,\cos(Kx - \Omega_L t - \Delta\,\sin(\Omega_P t))], \quad (1)$$

where I_0 is the average light intensity, K is the spatial frequency of the interference fringes, m is the effective contrast of the interference fringes, and Δ is the amplitude of the periodical modulation. Assuming small amplitudes of periodical modulation ($\Delta \ll 1$), the above expression can be simplified as follows:

$$I(x,t) = I_0\left\{1 + \frac{m}{2}\left[e^{i(Kx-\Omega_L t)} + \frac{\Delta}{2}\left(e^{i(Kx-\Omega_L t-\Omega_P t)} - e^{i(Kx-\Omega_L t+\Omega_P t)}\right) + c.c.\right]\right\}. \quad (2)$$

Note [Eq. (2)] that, in the absence of linear phase modulation ($\Omega_L = 0$), the oscillating interference pattern can be represented by superposition of three components: the stationary grating and two running in opposite direction with the equal speed gratings. If linear modulation is switched on ($\Omega_L \neq 0$), the stationary component does not exist anymore.

In the analysis we assume a p-type photoconductor with a single deep trapping center, where trap saturation is neglected. In addition, the lifetime of the mobile carriers is assumed to be negligibly small ($\tau \to 0$). Using the standard set of equations (given, e.g., in [1]) in approximation of small contrast ($m \ll 1$), the amplitude of the first harmonic of the ac photo-emf current density j^{Ω} for small spatial frequency of the interference fringes ($KL_D \ll 1$, where L_D is the photocarrier's diffusion length) and zero external dc field ($E_0 = 0$) can be obtained:

$$j^{\Omega} = -\frac{m^2\Delta}{2} K \frac{k_B T}{e} \sigma_0 \Omega_P \tau_{\mathrm{di}} \times \left(\frac{1 - \Omega_L^2 \tau_{\mathrm{di}}^2 + i\Omega_P \tau_{\mathrm{di}}}{(1+\Omega_L^2\tau_{\mathrm{di}}^2)(1+i(\Omega_L+\Omega_P)\tau_{\mathrm{di}})(1+i(\Omega_P-\Omega_L)\tau_{\mathrm{di}})} \right). \quad (3)$$

Here e is the elementary charge, T is the absolute temperature, k_B is the Boltzmann constant, σ_0 is the average photoconductivity, and $\tau_{\mathrm{di}} = \varepsilon\varepsilon_0/\sigma_0$ is the dielectric relaxation time, where $\varepsilon\varepsilon_0$ is the effective dielectric constant. The above analytical expression shows that, for arbitrary frequency $\Omega_P \neq \Omega_L$, the general effect of the continuous movement of the interference pattern is a decrease of the ac photo-emf signal amplitude [Figs. 1(b)–1(e)]. This fact is understandable, since, according to the standard (without a linear phase shift) theory of ac photo-emf effect, the magnitude of the output current depends on amplitudes of two interacting gratings induced by illuminating pattern—space charge electric field grating $E_{\mathrm{sc}}(x)$ and mobile carrier grating $p(x)$—as well as on a phase shift among them. The phase shift is optimized at high modulation frequency $\Omega_P \gg \tau_{\mathrm{di}}^{-1}$ when the space-charge-field grating, which is recorded/erased with the characteristic time τ_{di}, "sees" only the stationary component of oscillating interference pattern, while the free carriers are fast enough ($\tau \to 0$) to follow its oscillating components. As a consequence, the photo-emf signal is maximal, and it is independent on the frequency of periodical modulation [Fig. 1(a)]. In the presence of a linear phase shift, the stationary component of the interference pattern no longer exists, and therefore if the speed of displacement $V_L = \Omega_L/K$ is high enough (such as $\Omega_L \gg \tau_{\mathrm{di}}^{-1}$), the space charge electric field grating is effectively erased, producing a small photo-emf signal.

However, when the frequency of the periodical exitation Ω_P matches Ω_L ($\Omega_P = \Omega_L$), a sharp peak in the frequency dependence of the photo-emf signal can be observed (though the maximal signal amplitude experiences twofold decay as compared to the case of no frequency offset); see Figs. 1(b)–1(e). This peak occurs because at this condition the linear displacement is cancelled out by one of the running components of oscillating movement, and therefore a stationary component of illuminating pattern reappears as is shown by the fourth term of Eq. (2), which produces a large ac photo-emf current again.

The experiments reported here were performed in photo-emf reflectance configuration [8]. In addition to the conventional periodical phase modulation (driven by an electro-optic phase modulator) with a frequency Ω_P and amplitude $\Delta = 0.5$ rad, a linear phase shift in the signal beam was introduced by using two acousto-optical cells with a frequency offset $\Omega_{\mathrm{offset}} = \Omega_L$ between them. The photo-emf detector consists of a photoconductive polymer film (≈7 μm thickness) sandwiched between two glass plates covered by transparent indium tin oxide electrodes. The material for the detector was a mixture of the hole-conducting polymer poly-(*N*, *N*′-bis(4-hexylphenyl)-*N*′-(4-(9-phenyl-9H-fluoren-9-yl)phenyl)-4,4′-benzidine) (PF6:TPD) (49 wt. %) [9] doped with two azo dyes, 2,5-dimethyl-(4-*p*-nitrophenylazo)-anisole (DMNPAA) and 3-methoxy-(4-*p*-nitrophenylazo)-anisole (MNPAA) (25 wt. % each) and sensitized with the highly soluble C_{60} derivative PCBM (1 wt. %). Two counterpropagating beams derived from a cw He–Ne laser (λ = 633 nm) intersected inside the detector, creating an interference pattern with the spatial period $\Lambda = \lambda/(2\pi n) \approx 0.20$ μm ($n = 1.7$), effective contrast $m \approx 1$, and average light intensity $I_0 \approx 40$ mW/cm^2. The output photo-emf current J^{Ω} was detected as a voltage drop over a 100 KΩ load resistance by a lock-in amplifier.

The experimental data show (Fig. 2) that, without linear modulation, the ac photo-emf signal J^{Ω} can be considered as nearly frequency independent in the region 20 Hz $< \Omega_P/2\pi <$ 2 kHz.

The limits of this region, defined by these two characteristic frequencies, determine the detection bandwidth. The first characteristic frequency $\Omega_{P1}/2\pi$ grows linearly with light intensity, which allows us to associate this frequency to the dielectric relaxation process. The second frequency $\Omega_{P2}/2\pi$ is intensity independent, and it is related to the photoconductivity relaxation process [8]. When the linear modulation is introduced, the frequency dependence changes in a way predicted by the above theory: sharp signal peaks occur when two frequencies Ω_L and Ω_P match each other (Figs. 1 and 2). Thus, through the measurement of the position of this peak, the Doppler frequency shift Ω_L can be determined. Experimental dependencies of photo-emf current amplitude on frequency of modulation at different average light intensities I_0 are

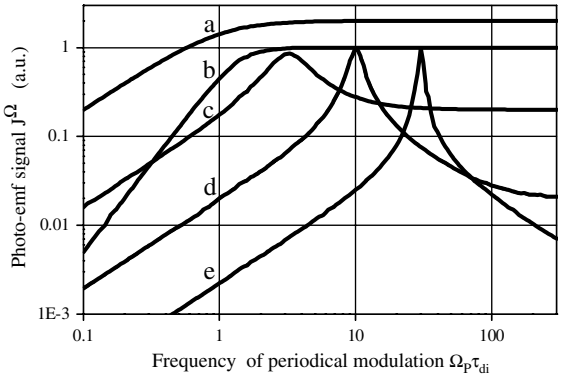

Fig. 1. Theoretical plot of photo-emf current J^{Ω} using Eq. (3) for different Ω_L. $\Omega_L\tau_{\mathrm{di}}$ = a, 0; b, 1; c, 3; d, 10; e, 30.

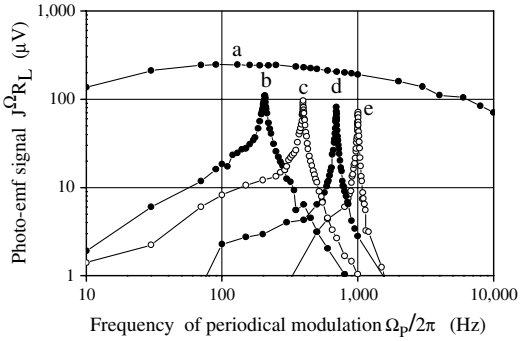

Fig. 2. Experimental dependence of photo-emf current J^{Ω} on the frequency of periodical modulation Ω_P for different Ω_L. $\Omega_L/2\pi$ = a, 0 Hz; b, 200 Hz; c, 400 Hz; d, 700 Hz; e, 1000 Hz.

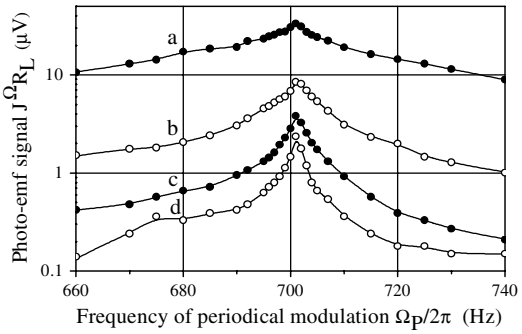

Fig. 3. Experimental dependence of non-steady-state photo-emf current J^{Ω} on the frequency of periodical modulation for different average light intensity I_0. I_0 = a, 40 mW/cm^2; b, 13 mW/cm^2; c, 6 mW/cm^2; d, 4 mW/cm^2 at $\Omega_L/2\pi = 700$ Hz.

shown in Fig. 3. In agreement with theoretical predictions [Eq. (3)], variations in I_0 change only the amplitude of the peak (it decays as I_0^{-1}), while its position remains unchanged. This renders the measurement of the linear frequency Ω_L intensity independent, which means that no additional calibration is needed. It is worth noting that, at low light intensity, the peak is better defined (i.e., it is narrower than the peaks at higher intensities). This can be explained by the slower dielectric relaxation time τ_{di} and as a consequence the more efficient erasure of the stable space-charge-field component at the frequencies that are different from Ω_L.

To prove the possibility to detect the Doppler frequency shift, the acousto-optical cells were removed, and one of the mirrors of the interferometer was attached to a calibrated loudspeaker driven by a periodical "sawtooth"-shaped voltage. Dependencies similar to that shown in Fig. 2 were observed, and evaluated velocities were found to be in good agreement with the values used to displace the mirror.

In summary, the non-steady-state photo-emf effect in the presence of both periodical and linear phase modulation was investigated. The feasibility to build a velocimeter based on this effect in a photoconductive polymer film was demonstrated. Such a velocimeter possesses two important advantages: simplicity of optical and electronic configuration (no need for calibration) and robustness to environmental vibrations. The drawback of this method relies on the fact that it is not a single shot measurement since the scan on frequency of periodical modulation must be performed. Therefore, the method requires a stable Doppler shift during the scanning and detector response time scale τ_{di}.

S. M. acknowledges Consejo Nacional de Ciencia y Tecnología project 84922 for financial support. S. K. and K. M acknowledge support from Bundesministerium für Bildung und Forschung (Deutsches Zentrum für Luft- und Raumfahrt 50WB0730).

References

1. S. Stepanov, in *Handbook of Advanced Electronic and Photonic Materials and Devices*, H. S. Nalwa, ed. (Academic, 2001), pp. 205–272.
2. P. Delaye and G. Roosen, in *IUTAM Symposium on Advanced Optical Methods and Applications in Solid Mechanics* (Springer Netherlands, 2006), pp. 401–408.
3. T. O. dos Santos, J. Frejlich, J. C. Launay, and K. Shcherbin, Appl. Phys. B **95**, 627 (2009).
4. C. C. Wang, F. Davidson, and S. Trivedi, J. Opt. Soc. Am. B **14**, 21 (1997).
5. M. P. Petrov, I. A. Sokolov, S. I. Stepanov, and G. S. Trofimov, J. Appl. Phys. **68**, 2216 (1990).
6. C. C. Wang, F. Davidson, and S. Trivedi, Appl. Opt. **34**, 6496 (1995).
7. C. C. Wang, R. A. Linke, D. D. Nolte, M. R. Melloch, and S. Trivedi, Appl. Phys. Lett. **70**, 2034 (1997).
8. M. C. Gather, S. Mansurova, and K. Meerholz, Phys. Rev. B **75**, 165203 (2007).
9. J. Schelter, G. F. Mielke, A. Köhnen, J. Wies, S. Köber, O. Nuyken, and K. Meerholz, Macromol. Rapid Commun. **31**, 1560 (2010).